Supporting information for: Extremely strong bipolar optical interactions between paired graphene nanoribbons

Wanli Lu,[*,†] Huajin Chen,[‡,¶] Shiyang Liu,[*,‡,§] Jian Zi,[‡,¶] and Zhifang Lin[*,‡,¶,‖]

Department of Physics, China University of Mining and Technology, Xuzhou, Jiangsu 221116, China, State Key Laboratory of Surface Physics and Department of Physics, Fudan University, Shanghai 200433, China, Key Laboratory of Micro and Nano Photonic Structures, Fudan University, Shanghai 200433, China, Institute of Information Optics, Zhejiang Normal University, Jinhua, Zhejiang 321004, China, and Collaborative Innovation Center of Advanced Microstructures, Fudan University, Shanghai 200433, China

E-mail: luwl@cumt.edu.cn; syliu@zjnu.cn; phlin@fudan.edu.cn

1 Dispersion relation of the double-layer graphene sheets

For the two dimensional double-layer graphene sheets, each single graphene layer with one atom thickness can be treated as a boundary with optical conductivity σ, and the whole space is separated into three regions, as illustrated in Figure S1. The corresponding x components

[*]To whom correspondence should be addressed
[†]Department of Physics, China University of Mining and Technology, Xuzhou, Jiangsu 221116, China
[‡]State Key Laboratory of Surface Physics and Department of Physics, Fudan University, Shanghai 200433, China
[¶]Key Laboratory of Micro and Nano Photonic Structures, Fudan University, Shanghai 200433, China
[§]Institute of Information Optics, Zhejiang Normal University, Jinhua, Zhejiang 321004, China
[‖]Collaborative Innovation Center of Advanced Microstructures, Fudan University, Shanghai 200433, China

of magnetic fields read

$$H_x = \begin{cases} H_1 \exp\left[\alpha_1\left(y+\frac{g}{2}\right)\right]\exp(i\beta z), & y < -g/2, \\ (H_a \cosh\alpha_g y + H_b \sinh\alpha_g y)\exp(i\beta z), & |y| \le g/2, \\ H_2 \exp\left[-\alpha_1\left(y-\frac{g}{2}\right)\right]\exp(i\beta z), & y > g/2, \end{cases} \tag{1}$$

where $\alpha_1^2 = \beta^2 - \epsilon_1 k_0^2$ and $\alpha_g^2 = \beta^2 - \epsilon_g k_0^2$.

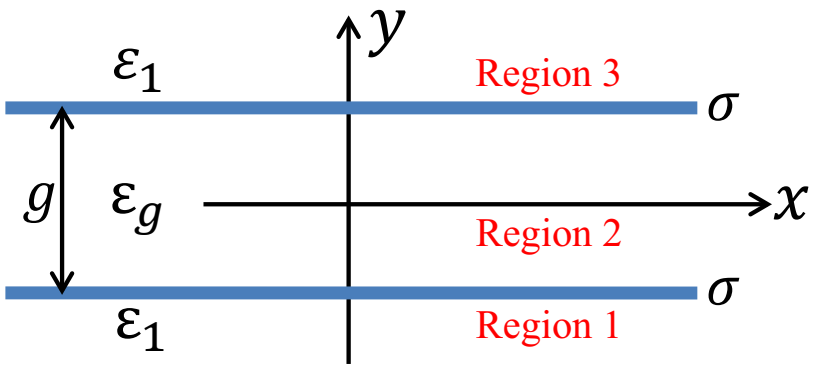

Figure S1: Sketch of the two dimensional double-layer graphene sheets.

By matching the boundary conditions at $y = \pm g/2$

$$\begin{aligned} H_{x1} - H_{x2} &= \sigma E_{z1}, \\ E_{z1} &= E_{z2}, \\ H_{x2} - H_{x3} &= \sigma E_{z3}, \\ E_{z2} &= E_{z3}, \end{aligned} \tag{2}$$

one has

$$\begin{aligned} H_1\frac{\alpha_1\epsilon_g}{\epsilon_1\alpha_g} &= -H_a \sinh\left(\alpha_g\frac{g}{2}\right) + H_b\cosh\left(\alpha_g\frac{g}{2}\right), \\ H_2\frac{\alpha_1\epsilon_g}{\epsilon_1\alpha_g} &= -H_a \sinh\left(\alpha_g\frac{g}{2}\right) - H_b\cosh\left(\alpha_g\frac{g}{2}\right), \\ H_1\left(1+\frac{i\alpha_1\sigma}{\epsilon_0\epsilon_1\omega}\right) &= H_a\cosh\left(\alpha_g\frac{g}{2}\right) - H_b\sinh\left(\alpha_g\frac{g}{2}\right), \\ H_2\left(1+\frac{i\alpha_1\sigma}{\epsilon_0\epsilon_1\omega}\right) &= H_a\cosh\left(\alpha_g\frac{g}{2}\right) + H_b\sinh\left(\alpha_g\frac{g}{2}\right). \end{aligned} \tag{3}$$

For the even mode, $H_1 = H_2$ is required so that we have

$$\begin{aligned} H_a &= -H_1 \frac{\alpha_1 \epsilon_g}{\epsilon_1 \alpha_g} \frac{1}{\sinh\left(\alpha_g \frac{g}{2}\right)}, \\ H_b &= 0, \end{aligned} \tag{4}$$

while $H_1 = -H_2$ in case of the odd mode, then

$$\begin{aligned} H_a &= 0, \\ H_b &= H_1 \frac{\alpha_1 \epsilon_g}{\epsilon_1 \alpha_g} \frac{1}{\cosh\left(\alpha_g \frac{g}{2}\right)}. \end{aligned} \tag{5}$$

As a result, the magnetic fields can be rewritten as

$$H_x = \begin{cases} H_1 \exp\left[\alpha_1 \left(y + \frac{g}{2}\right)\right] \exp(i\beta z), & y < -g/2, \\ -H_1 \frac{\alpha_1 \epsilon_g}{\epsilon_1 \alpha_g} \frac{\cosh \alpha_g y}{\sinh(\alpha_g g/2)} \exp(i\beta z), & |y| \leq g/2, \\ H_1 \exp\left[\alpha_1 \left(y - \frac{g}{2}\right)\right] \exp(i\beta z), & y > g/2, \end{cases} \tag{6}$$

for the even mode, and

$$H_x = \begin{cases} H_1 \exp\left[\alpha_1 \left(y + \frac{g}{2}\right)\right] \exp(i\beta z), & y < -g/2, \\ H_1 \frac{\alpha_1 \epsilon_g}{\epsilon_1 \alpha_g} \frac{\sinh \alpha_g y}{\cosh(\alpha_g g/2)} \exp(i\beta z), & |y| \leq g/2, \\ -H_1 \exp\left[\alpha_1 \left(y - \frac{g}{2}\right)\right] \exp(i\beta z), & y > g/2, \end{cases} \tag{7}$$

for the odd mode.

Based on eq 3 and further considering the characteristics of the even and odd modes in eqs 4 and 5, the dispersion relations can be retrieved with some simple mathematical manipulations

$$\begin{cases} \tanh\left(\alpha_g \frac{g}{2}\right) = \frac{i\alpha_1 \epsilon_0 \epsilon_g \omega}{\alpha_g(\alpha_1 \sigma - i\epsilon_0 \epsilon_1 \omega)}, & \text{even mode}, \\ \tanh\left(\alpha_g \frac{g}{2}\right) = -\frac{i\alpha_1 \alpha_g \sigma + \alpha_g \epsilon_0 \epsilon_1 \omega}{\alpha_1 \epsilon_0 \epsilon_g \omega}, & \text{odd mode}. \end{cases} \tag{8}$$

Let the factor

$$\Gamma = \frac{\alpha_g \epsilon_1}{\epsilon_g \alpha_1}\left(1 + i\frac{\alpha_1 \sigma}{\epsilon_0 \epsilon_1 \omega}\right), \tag{9}$$

then, the dispersion relations are cast into

$$\begin{cases} \tanh\left(\dfrac{\alpha_g g}{2}\right) = -\dfrac{1}{\Gamma}, & \text{even mode,} \\ \tanh\left(\dfrac{\alpha_g g}{2}\right) = -\Gamma, & \text{odd mode.} \end{cases} \tag{10}$$

2 Analytical formulae for the effective mode indices of the double-layer graphene sheets

Based on the obtained dispersion relations in eqs 8 and 10, the effective mode indices for both the even and odd modes can be obtained in terms of the definition $n_{\text{eff}} = \beta/k_0$. For the air background, $\epsilon_g = \epsilon_1 = 1$ and $\alpha_g = \alpha_1$, the dispersion relations can be rewritten as

$$\begin{cases} \tanh(t) = \dfrac{-1}{1 + i\dfrac{\alpha_1 \sigma}{\epsilon_0 \epsilon_1 \omega}}, & \text{even mode,} \\ \tanh(t) = -\left(1 + i\dfrac{\alpha_1 \sigma}{\epsilon_0 \epsilon_1 \omega}\right), & \text{odd mode,} \end{cases} \tag{11}$$

with $t = \alpha_1 g/2$. Due to the fact that $\Im[\alpha_1 g/2] \sim 0$ and $0 < \Re[\alpha_1 g/2] \ll 1$ for the strongly coupled optical fields in the concerned system, we thus have $\tanh(t) \approx t$ so that the dispersion relations can be simplified into

$$\begin{cases} t + 1 + 2i\dfrac{\sigma}{\epsilon_0 \omega g} t^2 = 0, & \text{even mode,} \\ t\left(1 + \dfrac{2i\sigma}{\epsilon_0 \omega g}\right) + 1 = 0, & \text{odd mode.} \end{cases} \tag{12}$$

By solving eq 12, we obtain

$$\begin{cases} t = i\dfrac{\epsilon_0 \omega g}{4\sigma} + \dfrac{\sqrt{\epsilon_0 \omega g}}{4\sigma}\sqrt{8i\sigma - \epsilon_0 \omega g}, & \text{even mode,} \\ t = \dfrac{-\epsilon_0 \omega g}{\epsilon_0 \omega g + 2i\sigma}, & \text{odd mode.} \end{cases} \tag{13}$$

For the doped graphene monolayer in the main text, the optical conductivity is given by

$$\sigma = \sigma_r + i\sigma_i = \frac{e^2 E_F}{\pi\hbar^2}\frac{i}{\omega + i\tau^{-1}}, \tag{14}$$

Taking into account the condition $\omega\tau \gg 1$, we can obtain the real and imaginary parts of the optical conductivity in simple forms

$$\begin{aligned} \sigma_r &\approx \frac{e^2 E_F}{\pi\hbar^2}\frac{\tau^{-1}}{\omega^2}, \\ \sigma_i &\approx \frac{e^2 E_F}{\pi\hbar^2}\frac{1}{\omega}, \end{aligned} \tag{15}$$

where $\sigma_i \gg \sigma_r$ in virtue of $\omega\tau \gg 1$. Then, the factors $(8i\sigma - \epsilon_0\omega g) = -(8\sigma_i + \epsilon_0\omega g) + 8i\sigma_r \approx -(8\sigma_i + \epsilon_0\omega g)$, $t = \alpha_1 g/2 \approx \beta g/2 = k_0 n_{\text{eff}} g/2$, and $\sigma \approx i\sigma_i$, we can obtain the real parts of the effective mode indices associated, respectively, with the even and odd modes

$$\begin{cases} \Re[n^b_{\text{eff}}] \approx \sqrt{C_1^2/g + C_0^2} + C_0, & \text{even mode}, \\ \Re[n^a_{\text{eff}}] \approx \dfrac{2C_0}{1 - C_0 k_0 g}, & \text{odd mode}, \end{cases} \tag{16}$$

where $Z_0 = \sqrt{\mu_0/\epsilon_0}$ is the wave impedance in vacuum, and the coefficients

$$\begin{aligned} C_0 &= \frac{k_0}{4}C_1^2 = \frac{\pi\hbar^2\omega}{2Z_0 e^2 E_F}, \\ C_1 &= \sqrt{\frac{2\pi}{\mu_0}}\frac{\hbar}{e}\frac{1}{\sqrt{E_F}}. \end{aligned} \tag{17}$$

To examine the approximations used in deriving the analytical formulae in eq 16, we calculate the real parts of effective mode indices as the functions of the gap distance for the system with the parameters of Figure 3 in the main text based on the analytical expressions, in comparison with the corresponding results obtained with the rigorous numerical calculation of eq 11. They are in perfect agreement with each other, as indicated by the blue dashed lines and green solid lines in Figure S2, justifying the analysis.

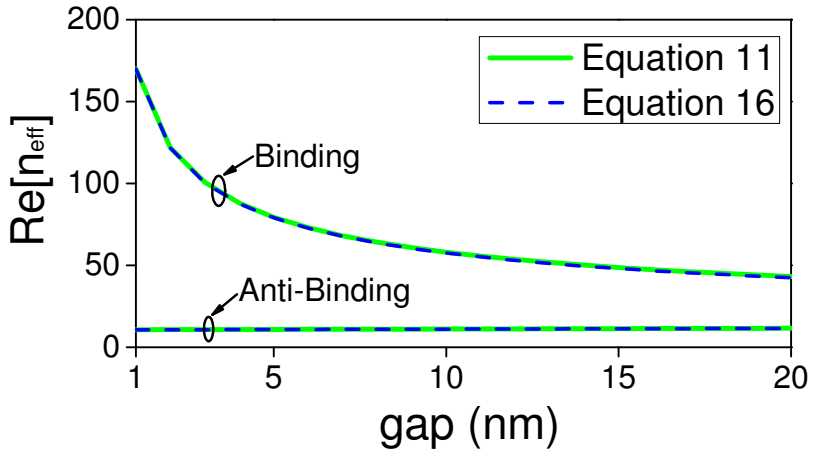

Figure S2: The real part of the effective mode indices versus the gap distance for the even mode (binding state) and the odd mode (anti-binding state).

3 Analytical formulae for the optical forces between the double-layer graphene sheets

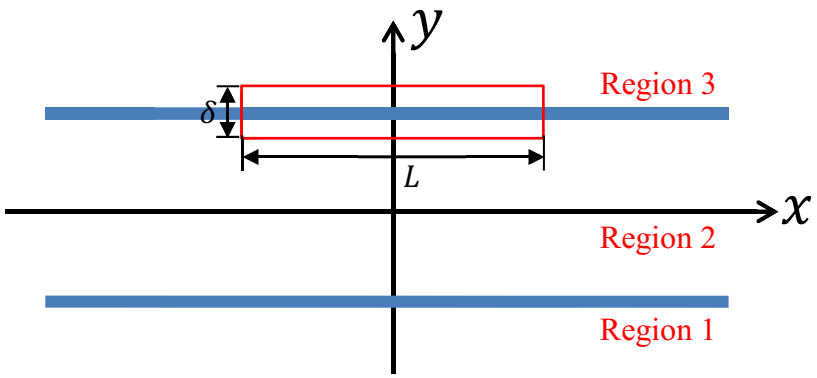

Figure S3: Sketch of the integral curve for the calculations of the optical binding and anti-binding forces. The red closed curve denotes the integral contour with the width L and the thickness δ.

The optical binding and anti-binding forces can also be calculated by use of the integral of the Maxwell's stress tensor along an arbitrary closed contour illustrated in Figure S3

$$\boldsymbol{f} = \oint_C \langle \bar{\bar{\mathbf{T}}} \rangle \cdot \mathrm{d}\mathbf{S}. \tag{18}$$

For the graphene monolayer, the optical forces per unit length read

$$\boldsymbol{f} = \int_L \mathrm{d}x\langle\bar{\bar{\mathbf{T}}}_3\rangle \cdot \boldsymbol{e}_y + \int_L \mathrm{d}x\langle\bar{\bar{\mathbf{T}}}_2\rangle \cdot (-\boldsymbol{e}_y) + \int_\delta \mathrm{d}y\langle\bar{\bar{\mathbf{T}}}\rangle \cdot \boldsymbol{e}_x + \int_\delta \mathrm{d}y\langle\bar{\bar{\mathbf{T}}}\rangle \cdot (-\boldsymbol{e}_x), \tag{19}$$

where δ is the thickness of the graphene layer, L is the width of the graphene layer in the closed integral contour, and $\langle\bar{\bar{\mathbf{T}}}_i\rangle$ is the time-averaged Maxwell's stress tensor in Region i (with $i = 2, 3$). Considering graphene plasmons of the TM mode (E_y, E_z, H_x), with $\delta \ll L$ and the independence of the field profile on x coordinate, the optical force is reduced to

$$\boldsymbol{f} = \langle\bar{\bar{\mathbf{T}}}_3\rangle \cdot \boldsymbol{e}_y L + \langle\bar{\bar{\mathbf{T}}}_2\rangle \cdot (-\boldsymbol{e}_y) L = \left(\langle\bar{\bar{\mathbf{T}}}_3\rangle - \langle\bar{\bar{\mathbf{T}}}_2\rangle\right) \cdot \boldsymbol{e}_y L. \tag{20}$$

Finally, the y component of optical forces can be expressed in a simpler form

$$f_y = \left(T_{yy}|_3 - T_{yy}|_2\right) L, \tag{21}$$

with

$$T_{yy}|_i = \frac{1}{4}\Re\left[\epsilon_0\epsilon_r|E_{yi}|^2 - \epsilon_0\epsilon_r|E_{zi}|^2 - \mu_0\mu_r|H_{xi}|^2\right]. \tag{22}$$

At the position $y = g/2$, the z component of the electric field E_z is continuous when crossing the interface from Region 3 to Region 2, so the term $|E_z|^2$ has no contribution to the optical forces. The optical force f_y can therefore be rewritten as

$$\begin{aligned} f_y &= \frac{L}{4}\Re\left[\epsilon_0\epsilon_{r3}|E_{y3}|^2 - \mu_0\mu_{r3}|H_{x3}|^2\right] - \frac{L}{4}\Re\left[\epsilon_0\epsilon_{r2}|E_{y2}|^2 - \mu_0\mu_{r2}|H_{x2}|^2\right] \\ &= \frac{\epsilon_0 L}{4}\left(|E_{y3}|^2\Re[\epsilon_{r3}] - |E_{y2}|^2\Re[\epsilon_{r2}]\right) - \frac{\mu_0 L}{4}\left(|H_{x3}|^2\Re[\mu_{r3}] - |H_{x2}|^2\Re[\mu_{r2}]\right). \end{aligned} \tag{23}$$

After using $E_y = -\frac{\beta}{\omega\epsilon_0\epsilon_r}H_x$ obtained from Maxwell's equations, for the non-magnetic background medium with $\mu_{r3} = \mu_{r2} = 1$, the optical force f_y is cast into

$$f_y = L\left(\frac{|\beta|^2\Re[\epsilon_{r3}]}{4\omega^2\epsilon_0|\epsilon_{r3}|^2} - \frac{\mu_0}{4}\right)|H_{x3}|^2 - L\left(\frac{|\beta|^2\Re[\epsilon_{r2}]}{4\omega^2\epsilon_0|\epsilon_{r2}|^2} - \frac{\mu_0}{4}\right)|H_{x2}|^2. \tag{24}$$

For the air background with $\epsilon_{r3} = \epsilon_{r2} = 1$, the optical force is further reduced to

$$\begin{aligned} f_y &= \frac{\mu_0 L}{4}\left(\frac{|\beta|^2}{k_0^2} - 1\right)\left(|H_{x3}|^2 - |H_{x2}|^2\right) \\ &= \frac{\mu_0 L}{4}\left(|n_{\text{eff}}|^2 - 1\right)\left(|H_{x3}|^2 - |H_{x2}|^2\right). \end{aligned} \tag{25}$$

Considering the fact that the effective mode indices of the double-layer graphene are much larger than one, when the H_x is strongly discontinuous, an extremely strong optical force can be obtained according to eq 25. As evidenced in Figure S4, we can see that the x component of magnetic fields in regions 2 and 3 exhibit dramatic discontinuity, concretely, $|H_{x3}| \ll |H_{x2}|$ for the even mode and $|H_{x3}| \gg |H_{x2}|$ for the odd mode. As a result, the attractive optical binding force is associated with the even mode, while the repulsive optical anti-binding force is associated with odd mode.

For the convenience of interpretation, the optical forces should be normalized by the total optical power P_z coupled into the double-layer graphene sheets with

$$P_z = L\int_{-\infty}^{-\frac{g}{2}} \langle S_{z1}\rangle \mathrm{d}y + L\int_{-\frac{g}{2}}^{\frac{g}{2}} \langle S_{z2}\rangle \mathrm{d}y + L\int_{\frac{g}{2}}^{\infty} \langle S_{z3}\rangle \mathrm{d}y, \tag{26}$$

where $\langle S_{zi}\rangle = \frac{1}{2\omega\epsilon_0}\Re[\frac{\beta}{\epsilon_{ri}}]|H_{xi}|^2$ is z component of the Poynting vector with $(i = 1, 2, 3)$, corresponding to three different regions. By dividing the optical force in eq 25 with the optical power in eq 26, we can obtain the normalized optical binding force associated with the even mode

$$F_y^b = \frac{f_y}{P_z} = -\frac{\left(\alpha_1^2 - \alpha_1^{*2}\right)\left(|\beta|^2 - k_0^2\right)\left(e^{\alpha_1^* g} + e^{\alpha_1 g}\right)}{4\omega\Re[\beta]\left(\alpha_1^* e^{\alpha_1 g} - \alpha_1 e^{\alpha_1^* g} + 2i e^{\alpha_1^* g} e^{\alpha_1 g}\Im[\alpha_1]\right)}, \tag{27}$$

and the normalized optical anti-binding force associated with the odd mode

$$F_y^a = -\frac{\left(\alpha_1^2 - \alpha_1^{*2}\right)\left(|\beta|^2 - k_0^2\right)\left(e^{\alpha_1^* g} + e^{\alpha_1 g}\right)}{4\omega\Re[\beta]\left(\alpha_1^* e^{\alpha_1 g} - \alpha_1 e^{\alpha_1^* g} - 2i e^{\alpha_1^* g} e^{\alpha_1 g}\Im[\alpha_1]\right)}. \tag{28}$$

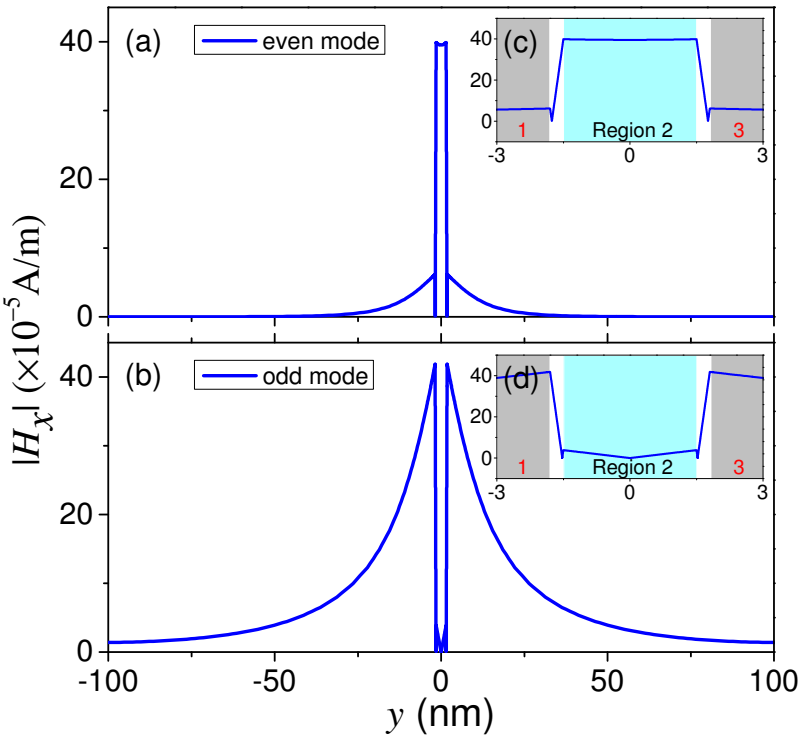

Figure S4: Absolute values of the x component of magnetic fields $|H_x|$ corresponding to the even (a) and odd (b) modes are plotted as the functions of y coordinate based on the FEM. All the other parameters are those used in the main text except the gap distance $g = 3$ nm. The insets are the amplified view of the field profiles for the even (c) and odd (d) modes in the region -3 nm$< y < 3$ nm, where three regions are marked with colored backgrounds, serving as the guide to the eye. The narrow whiteout regions in the insets denote the graphene layers.

With the identical relations $\Re[e^{A+iB}] = e^A \cos B$ and $\Im[e^{A+iB}] = e^A \sin B$, the optical binding and anti-binding forces can be rewritten as

$$\begin{cases} F_y^b = -\dfrac{(|\beta|^2 - k_0^2)\,\Re[\alpha_1]\Im[\alpha_1]e^{Re[\alpha_1]g}\cos(\Im[\alpha_1]g)}{\omega\Re[\beta]\,(\Im[\alpha_1^* e^{\alpha_1 g}] + \Im[\alpha_1]e^{2\Re[\alpha_1]g})}, & \text{even modes,} \\ F_y^a = -\dfrac{(|\beta|^2 - k_0^2)\,\Re[\alpha_1]\Im[\alpha_1]e^{Re[\alpha_1]g}\cos(\Im[\alpha_1]g)}{\omega\Re[\beta]\,(\Im[\alpha_1^* e^{\alpha_1 g}] - \Im[\alpha_1]e^{2\Re[\alpha_1]g})}, & \text{odd modes.} \end{cases} \tag{29}$$

Considering $\Im[\alpha_1^* e^{\alpha_1 g}] = \Im[\alpha_1^*]\Re[e^{\alpha_1 g}] + \Re[\alpha_1^*]\Im[e^{\alpha_1 g}]$, $\Im[\alpha_1^*] = -\Im[\alpha_1^*]$, and $\Re[\alpha_1^*] = \Re[\alpha_1^*]$,

the factors $\Im[\alpha_1^* e^{\alpha_1 g}] \pm \Im[\alpha_1] e^{2\Re[\alpha_1]g}$ in the denominators of eq 29 become

$$\begin{aligned} I &\equiv \Im[\alpha_1^* e^{\alpha_1 g}] \pm \Im[\alpha_1] e^{2\Re[\alpha_1]g} \\ &= \Im[\alpha_1] \left(\pm e^{2\Re[\alpha_1]g} - \Re[e^{\alpha_1 g}] \right) + \Re[\alpha_1] e^{\Re[\alpha_1]g} \sin(\Im[\alpha_1] g) \\ &= \Re[\alpha_1] e^{\Re[\alpha_1]g} \sin(\Im[\alpha_1] g) \pm \Im[\alpha_1] \left(\mp e^{\Re[\alpha_1]g} \cos(\Im[\alpha_1] g) + e^{2\Re[\alpha_1]g} \right) \\ &= \left[\Re[\alpha_1] \sin(\Im[\alpha_1] g) \pm \Im[\alpha_1] \left(e^{\Re[\alpha_1]g} \mp \cos(\Im[\alpha_1] g) \right) \right] e^{\Re[\alpha_1]g}, \end{aligned} \tag{30}$$

then, the optical binding and anti-binding forces read

$$\begin{cases} F_y^b = -\dfrac{(|\beta|^2 - k_0^2)\, \Re[\alpha_1] \Im[\alpha_1] \cos(\Im[\alpha_1] g)}{\omega \Re[\beta] \left[\Re[\alpha_1] \sin(\Im[\alpha_1] g) + \Im[\alpha_1] \left(e^{\Re[\alpha_1]g} - \cos(\Im[\alpha_1] g) \right) \right]}, & \text{even mode,} \\ F_y^a = -\dfrac{(|\beta|^2 - k_0^2)\, \Re[\alpha_1] \Im[\alpha_1] \cos(\Im[\alpha_1] g)}{\omega \Re[\beta] \left[\Re[\alpha_1] \sin(\Im[\alpha_1] g) - \Im[\alpha_1] \left(e^{\Re[\alpha_1]g} + \cos(\Im[\alpha_1] g) \right) \right]}, & \text{odd mode.} \end{cases} \tag{31}$$

Because $\Im[\alpha_1] g \ll 1$, $k_0^2 \ll |\beta|^2$ and $\Im[\beta] \ll \Re[\beta]$, $\cos(\Im[\alpha_1] g) \approx 1$, and $\sin(\Im[\alpha_1] g) \approx \Im[\alpha_1] g$, the optical binding and anti-binding forces can be simplified into

$$\begin{aligned} F_y^b &\approx -\frac{|\beta|^2 \Re[\alpha_1] \Im[\alpha_1]}{\omega \Re[\beta] \left[\Re[\alpha_1] \Im[\alpha_1] g + \Im[\alpha_1] \left(e^{\Re[\alpha_1]g} - 1 \right) \right]} \\ &\approx -\frac{\Re[n_{\text{eff}}]}{c} \frac{\Re[\alpha_1]}{\Re[\alpha_1] g + \left(e^{\Re[\alpha_1]g} - 1 \right)}, \end{aligned} \tag{32}$$

and

$$\begin{aligned} F_y^a &\approx -\frac{|\beta|^2 \Re[\alpha_1] \Im[\alpha_1]}{\omega \Re[\beta] \left[\Re[\alpha_1] \Im[\alpha_1] g - \Im[\alpha_1] \left(e^{\Re[\alpha_1]g} + 1 \right) \right]} \\ &\approx -\frac{\Re[n_{\text{eff}}]}{c} \frac{\Re[\alpha_1]}{\Re[\alpha_1] g - \left(e^{\Re[\alpha_1]g} + 1 \right)}. \end{aligned} \tag{33}$$